Journal of Communications Technology and Electronics, Vol. 49, No. 12, 2004, pp. 1405–1410. Translated from Radiotekhnika i Elektronika, Vol. 49, No. 12, 2004, pp. 1507–1513.

MICROWAVE ELECTRONICS

Synchronization of a Beam–Backward-Wave System Having Cubic Phase Nonlinearity

A. E. Hramov

Received June 3, 2003

Abstract—A computer simulation is reported concerning the synchronization of a beam–backward-wave distributed active medium in which bunching takes place in the RF field, as found in the transverse-field backward-wave oscillator. The space-charge wave is assumed to have cubic phase nonlinearity. Synchronous operation and loss of synchronism are examined. The transient behavior of the driven oscillator is contrasted with that of previously studied backward-wave devices using drift-space bunching.

INTRODUCTION

There is great interest in the synchronization of distributed self-sustaining systems found in microwave vacuum electronics. It is especially important to consider the phenomenon in the context of backward-wave devices, for these make very useful and promising microwave sources varying in output power [1–4]. A number of investigations have been conducted into synchronization of the O-type backward-wave oscillator[1] (O-BWO) and the gyrotron backward-wave oscillator (gyro-BWO), in which a sinusoidal driving signal is injected at the collector end [5–12]. A basic understanding was thus gained of the synchronization and other features of spatial-pattern dynamics in driven beam–wave systems involving a backward wave. The models of the gyro- and the O-BWO employed so far tend to presume that the nonlinear amplitude limiting is mainly due to drift-space bunching [1–4, 6–11]. (In fact, this is the only mechanism of amplitude limiting for O-BWOs.) The driven behavior of such a beam–wave system was studied in detail [5–12]. On the other hand, amplitude limiting may also result from nonlinear variation in the phase of the space-charge wave. This is caused by lack of isochronism between oscillating electrons, frequency being a function of oscillator energy. The phase nonlinearity is related to bunching in the radio-frequency (RF) field. The second mechanism of amplitude limiting is also observed in gyro-BWOs, yet it is significant only at a small departure from isochronism [4]. We see that the phase nonlinearity of space-charge waves is an important factor in the synchronization of backward-wave devices. The simplest model of phase nonlinearity is cubic nonlinearity [4, 14, 15]. It corresponds to the transverse-field backward-wave oscillator (TFBWO) [16]. This is the simplest known beam–wave system that displays complicated self-sustaining oscillations [4]. Research into the synchronization of the device should improve our knowledge of the dynamics of driven active media involving a backward wave.

In view of the above, the aim of this work is to numerically investigate the driven dynamics of an electron beam subject to bunching in a backward electromagnetic wave. The beam–wave system is treated within the model of cubic phase nonlinearity, as found in the TFBWO.

MATHEMATICAL MODEL

Let us consider the interaction between a space-charge wave and a backward electromagnetic wave that are free from dispersion. In a linear approximation, the waves are described by the evolution equations

$$\frac{\partial F}{\partial \tau} - \frac{\partial F}{\partial \xi} = -AI, \tag{1}$$

$$\frac{\partial I}{\partial \tau} + \frac{\partial I}{\partial \xi} = -AF, \tag{2}$$

where $F = |F|\exp[j\varphi_F]$ and $I = |I|\exp[\varphi_I]$ are the dimensionless wave amplitudes that refer to the RF field and the electrons, respectively, and vary slowly with time over the interaction region; τ is dimensionless time; ξ is the dimensionless longitudinal coordinate; and A is the coupling parameter, which can be regarded as the dimensionless length of the system [4].

It can be shown that Eqs. (1) and (2) imply absolute instability [17]. The system should pass to steady-state oscillation due to nonlinear phenomena occurring in the space-charge wave. The simplest phenomenon is the departure from isochronism between oscillating electrons, which makes φ_I vary in a nonlinear manner. If the electrons follow identical trajectories, the energy W is related to the energy of the space-charge wave as

$$W = \alpha I^2, \tag{3}$$

[1] In particular, attention was given to the effect of beam premodulation on oscillation [5, 13].

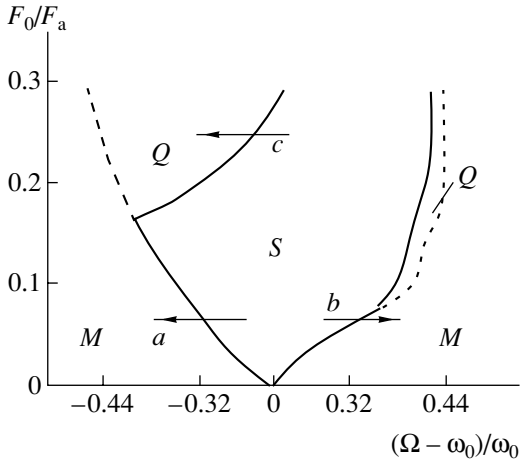

Fig. 1. Driving-parameter plane partitioned according to oscillation regimes, with F_a denoting the steady-state amplitude in the absence of driving. The solid curve is the boundary of the region of synchronism. The dashed curves refer to the locking of carrier frequency to driving frequency. Notice that quasi-synchronism is possible only at sufficiently large driving amplitudes.

where α is a coefficient of proportionality [4, 15]. Assume that, to a first approximation, the term of φ_I that varies as ξ is a linear function of energy. Then, changing to the coordinates $\tau' = (\tau - \xi)/2$ and $\xi' = \xi$ transforms Eq. (2) into

$$\partial I/\partial\xi + j|I|^2 I = -AF \qquad (4)$$

with the primes omitted. Equation (4) is subject to the boundary condition $I(\xi = 0, \tau) = 0$. This means that the space-charge wave vanishes at the gun end of the interaction region.

Equation (4) contains only one nonlinear term, which represents cubic nonlinearity due to the phase variation with longitudinal electron velocity. This decreases as the electron kinetic energy converts to radiation. Equation (1) remains unchanged. It is effectively the time-dependent equation of a transmission line excited by the current I that is given by Eq. (4).

Equations (1) and (4) constitute a simple model of the beam–wave system with phase nonlinearity. Its simplicity is due to the fact that all electron trajectories in the interaction region can be considered identical. This is not the case in O- and gyro-BWOs, which employ drift-space bunching [4, 15, 16, 18]. The fact that all electron oscillator trajectories are identical provides for a simple description of the electron wave dynamics.

Undriven dynamics associated with Eqs. (1) and (4) are known in detail [16, 19]. For $\pi/2 < A < 1.83$, the system produces sinusoidal oscillations with nonuniform $F(\xi)$ and $I(\xi)$. At $A > 1.83$, nonsinusoidal periodic oscillation occurs. In particular, when $A > 2.05$, the output field $F(\tau, \xi = 0)$ follows a pulsed pattern with faint ringing between the pulses. The ringing can be attributed to the multihumped shapes of $F(\xi)$ and $I(\xi)$, which should result from sharp and nonlinear variation of the space-charge phase over the interaction region. Finally, for $A > 4.5$, chaotic oscillations are excited. It has been noted that the route to chaos in the TFBWO resembles the period-doubling and period-adding routes in systems having a small number of degrees of freedom [15]. In this study, we investigated how self-sustaining oscillations in the TFBWO are affected by a sinusoidal driving signal of amplitude F_0 and frequency Ω injected at the collector end:

$$F(\xi = 1, \tau) = F_0 \exp[j\Omega\tau]. \qquad (5)$$

The device was assumed to operate at $A = 1.7$ (steady-state conditions). The driving frequency was measured in relation to the rest frequency.

SIMULATION RESULTS AND DISCUSSION

Below we present and discuss the results of a computer simulation concerned with the driven behavior of the TFBWO. The simulation was conducted within the time-dependent model using the cubic phase nonlinearity that was described in the preceding section. Equations (1)–(4) were solved by the Lax–Wendroff scheme and a second-order Runge–Kutta procedure, respectively, accurately to the second order. The spatial grid had $N = 500$ nodes, the mesh width being $\Delta\xi = 0.002$. The time step was set to $\Delta t = \Delta\xi/2 = 0.001$ so as to ensure computational stability. With the above methods and parameter values, we were able to accurately examine complex oscillation regimes and transients.

Figure 1 shows a driving-parameter plane partitioned according to main oscillation regimes. The parameters are F_0/F_a and $(\Omega - \omega_0)/\omega_0$, where F_a and ω_0 are the output amplitude and frequency, respectively, in the absence of driving.

If $\Omega/\omega_0 \sim 1.0$, the oscillator exhibits a synchronous regime, in which the output frequency ω is equal to the driving frequency and the output amplitude $|F(\xi = 0, \tau)|$ is a constant (after steady-state conditions have been reached). The synchronous regime is represented by the S region of Fig. 1. Once the representative point has left the S region, the amplitude $F(\xi = 0, \tau)$ starts to vary periodically with τ, so that $|F(\xi = 0, \tau)| = \text{const}$.

At certain values of the control parameters, the synchronization region boundary is crossed (the solid curve in Fig. 1). Then, the system starts operating so that the output field is modulated and the amplitude $|F(\xi = 0, \tau)|$ is a periodic function of time. On the regime map symbols Q and M refer to the regions of the output field periodic modulation.

This modulation is represented by the Q and M regions of Fig. 1. The Q and M regimes differ in the following respect. In the Q regime, the carrier frequency

of the output RF field is equal to Ω, and the output amplitude $|F|$ varies on the timescale $T_A \ll 2\pi/\Omega$. This regime will be referred to as quasi-synchronism [9–11, 20, 21].

The *M* regime is characterized by a carrier frequency which deviates from the driving frequency. Nevertheless, the output field amplitude varies slowly and periodically with time, analogous with the beating in driven oscillators which have a small number of degrees of freedom [22, 23]. Two interesting points can be made about the driven dynamics of the TFBWO as contrasted with that of gyro- and O-BWOs [9–11, 20, 21].

First, the shape of the *S* region is far more complex in our case. As F_0 is increased, the part below the level F_0/F_a loses symmetry, a property characteristic of gyro-BWOs [9, 10, 20, 21] and O-BWOs [11] under similar conditions. In Fig. 1, we also notice saturation in the edge corresponding to positive initial frequency detunings. Second, quasi-synchronism is a threshold phenomenon in terms of driving amplitude, the threshold value of $(F_0/F_a)^2$ being 0.01 to 0.02. (The regime is characterized by fairly complex and slow variation in $|F(\xi = 0, \tau)|$.) By contrast, gyro- and O-BWOs may show quasi-synchronism however small the driving amplitude [9–11, 20].

The *Q* region of the TFBWO (Fig. 1) differs markedly in structure from that of O- and gyro-BWOs. In particular, it includes a part corresponding to $(\Omega - \omega_0) < 0$, whose width grows rapidly with driving amplitude. At such driving parameters, both the bunched beam and the RF field exhibit amplitude modulation.

Figure 2 shows how the final frequency detuning $(\omega - \Omega)$ varies with $(\Omega - \omega_0)/\omega_0$ at different values of F_0. The condition $(\omega - \Omega) = 0$ corresponds to the *Q* or the *S* regime (the latter is confined to a certain frequency range). Notice that the region of quasi-synchronism is not symmetrical about $\Omega = \omega_0$ while F_0 remains small (curves *2*, *3*). As F_0 is increased, the region of synchronism becomes symmetrical, unlike what is observed in undriven gyro-BWOs under steady-state conditions [10, 20].

The features of the *S* and *Q* regimes also affect the ways in which the oscillator passes from these regimes to nonsynchronous operation. Figures 3a and 3b depict the frequency f_A and the period T_A of amplitude modulation for the output RF field as functions of negative or positive initial fractional frequency detuning, respectively, as the oscillator is brought deep into the nonsynchronous region, at $F_0/F_a = 0.1$ (see also Fig. 1). We notice that the transitions differ significantly from each other. With negative detunings, f_A grows from zero with the absolute value of detuning, and T_A decreases from infinity (Fig. 3a). With positive detunings, f_A (and hence T_A) varies in the reverse direction, and amplitude modulation arises with a finite f_A (Fig. 3b). Figures 4–6 illustrate how the output waveform $F(\xi = 0, \tau)$ changes during the transitions *a*, *b*, and *c* of Fig. 1, respectively, the time curves in each case being computed for three different driv-

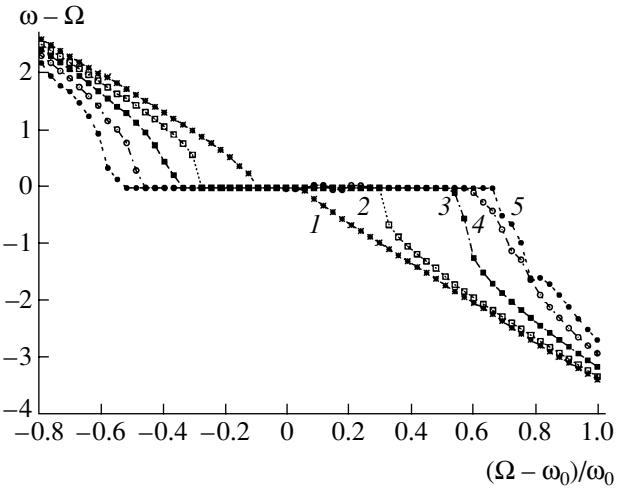

Fig. 2. Final frequency detuning vs. initial fractional frequency detuning for different normalized driving amplitudes: F_0/F_a = (*1*) 0.02, (*2*) 0.04, (*3*) 0.06, (*4*) 0.08, (*5*) 0.10.

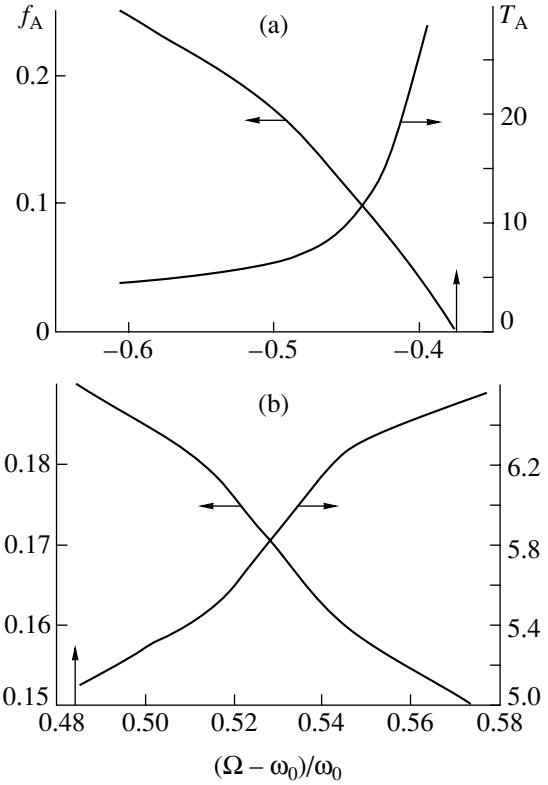

Fig. 3. The frequency and period of amplitude modulation vs. (a) negative or (b) positive initial fractional frequency detuning as the oscillator is brought deep into the nonsynchronous region at a normalized driving amplitude of $F_0/F_a = 0.1$ (the thick arrow marks loss of synchronism).

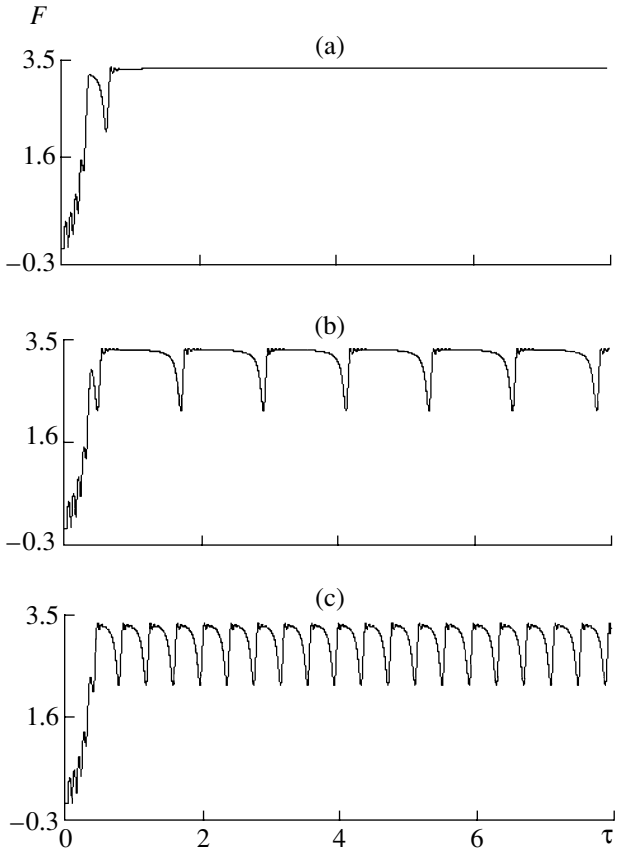

Fig. 4. Transition *a* of Fig. 1: changes in the output amplitude waveform $F(\xi = 0, \tau)$. The panels are computed for $(\omega_0 - \Omega)/\omega_0$ = (a) –0.36, (b) –0.34, (c) –0.46. The driving amplitude is fixed.

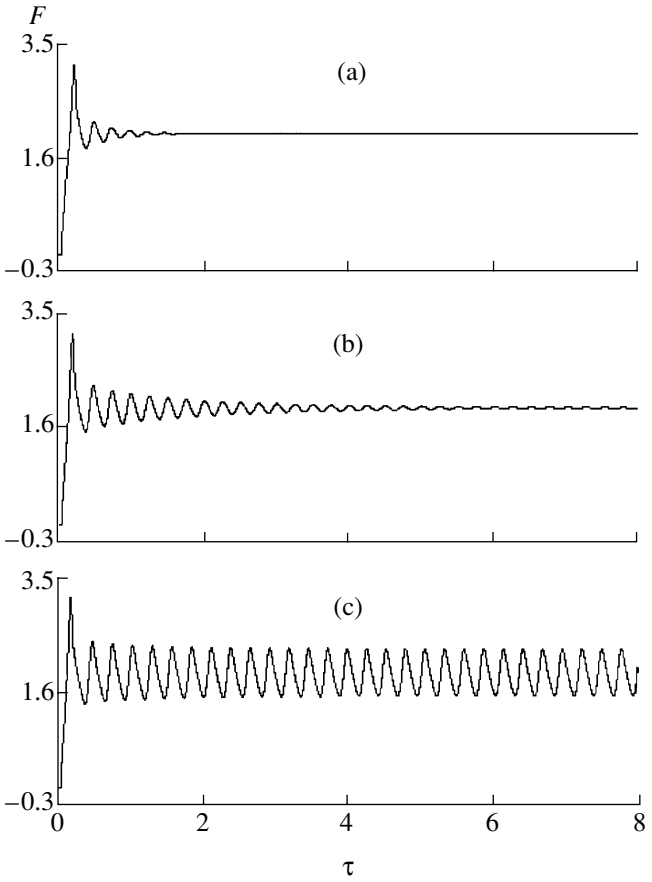

Fig. 5. Transition *b* of Fig. 1: changes in the output amplitude waveform $F(\xi = 0, \tau)$. The panels are computed for $(\Omega - \omega_0)/\omega_0$ = (a) 0.42, (b) 0.48, (c) 0.51. The driving amplitude is fixed.

ing frequencies. Figure 4 represents loss of synchronism at negative initial frequency detunings. In the *S* regime (Fig. 4a), the system experiences a short and complex transient to constant-amplitude oscillation at the driving frequency. The dynamics of the field spatial pattern indicate that the transient oscillation involves mode competition and the steady-state field amplitude is somewhat larger than the amplitude in the absence of driving.

Once driving has left the region of synchronism, the output field exhibits pulsed amplitude modulation (Fig. 4b). The pulses are characterized by a short leading edge, a wide plateau, and a long trailing edge. As the frequency detuning is increased in absolute value, the pulses narrow but retain their shape (the modulation period decreases) (Fig. 4c).

Figure 5 corresponds to positive initial frequency detunings. It is seen that the transition proceeds in a different manner. In the *S* regime the transient involves only one mode and appears as damped oscillations at a frequency f_t. The process becomes progressively longer as the detuning approaches the edge of the *S* region (Figs. 5a, 5b). Once the edge has been crossed, the system changes to undamped amplitude oscillations with $f_A \approx f_t$. At the edge, the modulation amplitude and frequency have nonzero finite values.

If the driving amplitude is taken to be large enough, the system passes to the *Q* regime (see above) as the detuning is increased, so that we again obtain undamped amplitude oscillations.

Comparing Figs. 4 and 5, we notice that the output RF amplitude is much larger in the case of negative initial frequency detunings. Accordingly, coupling in the *S* regime should be far more efficient when the driving frequency is less than the rest frequency, as with other backward-wave devices. (See monograph [5] and references therein for details of the phenomenon in *O*- and *M*-type backward-wave oscillators; a gyro-BWO under distributed driving via coupled transmission lines was addressed in [24].)

Figure 6 illustrates a transition to quasi-synchronism at a sufficiently large driving amplitude, indicated by arrow *c* in Fig. 1, in which case the system passes to an amplitude-modulated oscillation whose carrier fre-

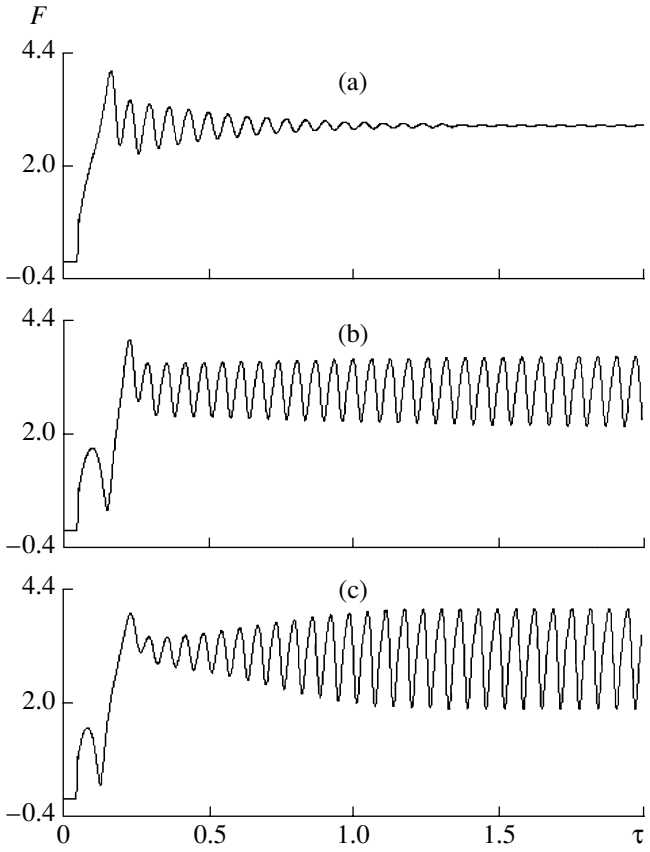

Fig. 6. Transition *c* of Fig. 1: changes in the output amplitude waveform $F(\xi = 0, \tau)$. The panels are computed for $(\Omega - \omega_0)/\omega_0$ = (a) 0, (b) –0.12, (c) –0.21. The normalized driving amplitude is set to $F_0/F_a = 0.25$. The oscillator passes from (a) synchronism to (b, c) quasi-synchronism.

quency is locked to the driving frequency. The waveforms $F(\xi = 0, \tau)$ show that the transition is qualitatively similar to that of Fig. 5. As the driving frequency is decreased, damping disappears and the waveform $|\Omega - \omega_0|$ assumes a pattern corresponding to a closed trajectory in the phase space (Figs. 6a–6c). We also observe a progressively increasing amount of amplitude modulation.

CONCLUSIONS

We investigated the effect of sinusoidal driving on self-sustaining oscillations in a backward-wave device in which bunching takes place in the RF field. The study was based on a computer simulation in terms of cubic phase nonlinearity. It has been established that the system may exhibit synchronism or quasi-synchronism, depending on parameters of nonlinearity and driving. (At synchronism the system oscillates at the driving frequency; at quasi-synchronism, it produces amplitude-modulated oscillation whose carrier frequency is equal to the driving frequency.) It has also been shown that the dynamics of the beam–wave system are broadly similar to those observed in our earlier studies of gyro- and O-BWOs, which mainly employ drift-space bunching [9–11, 20]. At the same time, the device concerned differs from the previous ones in the following important respects. First, quasi-synchronism is a threshold phenomenon: it arises only at a considerable driving amplitude. Second, the region of quasi-synchronism in the driving-parameter plane has a far more complex, asymmetrical shape. Note also that there are different routes from synchronism to amplitude modulation, depending on driving frequency and amplitude.

ACKNOWLEDGMENTS

The author is grateful to D.I. Trubetskov and A.A. Koronovskii for interest in this work and for helpful discussions and comments. This work was funded by the Russian Foundation for Basic Research (project no. 02-02-16351), the US Civilian Research & Development Foundation for the Independent States of the Former Soviet Union (CRDF, grant no. REC-006), the Dynasty Federal Scientific Program, and the MTsTsFM.

REFERENCES

1. *Backward-Wave Electronics*, Ed. by V. N. Shevchik and D. I. Trubetskov, (Saratov Gos. Univ., Saratov, 1978) [in Russian].
2. D. I. Trubetskov and A. E. Hramov, *Lectures on Microwave Electronics for Physicists* (Nauka, Moscow, 2003), Vol. 1 [in Russian].
3. K. L. Felch, B. G. Danly, H. R. Jory, *et al.*, Proc. IEEE **87**, 752 (1999).
4. D. I. Trubetskov and A. P. Chetverikov, Izv. Vyssh. Uchebn. Zaved., Prikl. Nelin. Din. **2** (5), 3 (1994).
5. B. E. Zhelezovskii and E. V. Kal'yanov, *Multifrequency Regimes of Microwave Devices* (Svyaz', Moscow, 1978) [in Russian].
6. G. P. Rapoport, Radiotekh. Elektron. (Moscow) **9**, 118 (1964).
7. V. A. Solntsev, Elektron. Tekh., Ser. Elektron. SVCh, No. 9, 30 (1966).
8. C. S. Kou, S. H. Chen, L. R. Barnett, *et al.*, Phys. Rev. Lett. **70**, 924 (1993).
9. D. I. Trubetskov and A. E. Hramov, Izv. Ross. Akad. Nauk, Ser. Fiz. **66**, 1761 (2002).
10. A. A. Koronovskii, D. I. Trubetskov, and A. E. Hramov, Izv. Vyssh. Uchebn. Zaved., Radiofiz. **45**, 773 (2002).
11. A. E. Hramov, Radiotekh. Elektron. (Moscow) **49**, 859 (2004) [J. Commun. Technol. Electron. **49**, (2004)].
12. A. A. Koronovskii, D. I. Trubetskov, and A. E. Hramov, Dokl. Akad. Nauk **389** (6), 1 (2003) [Dokl. Phys. **48**, 166 (2003)].
13. V. I. Kanavets, Vestn. Mosk. Univ., Ser. 3: Fiz., Astron., No. 2, 32 (1961).

14. A. P. Chetverikov, Izv. Ross. Akad. Nauk, Ser. Fiz. **58** (8), 171 (1994).

15. A. P. Chetverikov, Izv. Vyssh. Uchebn. Zaved., Prikl. Nelin. Din. **2** (5), 46 (1994).

16. S. P. Kuznetsov and A. P. Chetverikov, Izv. Vyssh. Uchebn. Zaved., Radiofiz. **24**, 109 (1981).

17. E. M. Lifshits and L. P. Pitaevskii, *Physical Kinetics* (Nauka, Moscow, 1979; Pergamon, Oxford, 1981).

18. S. P. Kuznetsov and A. P. Chetverikov, Radiotekh. Elektron. (Moscow) **23**, 385 (1978).

19. N. B. Frolova and A. P. Chetverikov, Izv. Vyssh. Uchebn. Zaved., Prikl. Nelin. Din. **10** (5), 50 (2002).

20. D. I. Trubetskov and A. E. Hramov, Pis'ma Zh. Tekh. Fiz. **28** (18), 34 (2002) [Tech. Phys. Lett. **28**, 767 (2002)].

21. A. E. Hramov, A. A. Koronovskii, and D. I. Trubetskov, in *Proceedings of the Fourth IEEE International Vacuum Electron Source Conference (IVESC'2002), Saratov, Russia, 2002*, p. 373.

22. M. I. Rabinovich and D. I. Trubetskov, *Introduction to the Theory of Oscillations and Waves* (RKhD, Izhevsk, 2000) [in Russian].

23. A. P. Kuznetsov, S. P. Kuznetsov, and N. M. Ryskin, *Nonlinear Oscillations* (Fizmatlit, Moscow, 2002) [in Russian].

24. A. A. Koronovskii and A. E. Hramov, Pis'ma Zh. Tekh. Fiz. **29** (12), 54 (2003) [Tech. Phys. Lett. **29**, 510 (2003)].